

# Prospection and Monitoring of the Archaeological Heritage of Nasca, Peru, with ENVISAT ASAR

**DEODATO TAPETE<sup>1\*</sup>, FRANCESCA CIGNA<sup>2</sup>, NICOLA MASINI<sup>3,5</sup> AND ROSA LASAPONARA<sup>4,5</sup>**

<sup>1</sup> Institute for the Conservation and Valorization of Cultural Heritage, National Research Council, Via Madonna del Piano 10, I-50019, Sesto Fiorentino, Florence, Italy

<sup>2</sup> British Geological Survey, Natural Environment Research Council, Nicker Hill, Keyworth, Nottingham, NG12 5GG, United Kingdom

<sup>3</sup> Institute for Archaeological and Monumental Heritage, National Research Council, Contrada S. Loja, I-85050, Tito Scalo, Potenza, Italy

<sup>4</sup> Institute of Methodologies for Environmental Analysis, National Research Council, Contrada S. Loja, I-85050, Tito Scalo, Potenza, Italy

<sup>5</sup> Italian mission of heritage Conservation and Archaeogeophysics (ITACA) in Peru

## ABSTRACT

The processing method based on synthetic aperture radar (SAR) amplitude information presented by Cigna et al. (2013, this issue) was used to extract the backscattering coefficient ( $\sigma^0$ ) from ENVISAT advanced SAR (ASAR) scenes to investigate the archaeological heritage of the Nasca region, southern Peru. Average backscattering and  $\sigma^0$  time series in 2003–2007 were obtained for some of the most famous groups of the Nazca Lines, as well as for the adobe structures of the Ceremonial Centre of Cahuachi, and allowed the recognition of anthropogenic features on arid and bare soil. Despite the expected constraints due to the medium spatial resolution of the ASAR scenes (~30 m), some features related to the Nasca ancient aqueduct systems (*puquios*) were detected, and water level changes were inferred from amplitude change detection maps and  $\sigma^0$  time series. The SAR-based prospection results were also compared with a vegetation index derived from Advanced Spaceborne Thermal Emission and Reflection Radiometer (ASTER) data for 2003, 2004 and 2007. The changes observed over Cahuachi and the neighbouring archaeological mounds are then discussed in light of the recent conservation history of the site and the contemporary archaeological excavations. The research opens interesting perspectives for routine use of SAR data for purposes of archaeological prospection and condition monitoring in (semi-)arid and desert regions. Copyright © 2013 John Wiley & Sons, Ltd.

**Key words:** Archaeological prospection; SAR processing; backscattering coefficient; change detection; Nasca; Peru

## Introduction

The cultural and natural richness of the Nasca region, southern Peru (Figure 1a), is not as yet fully discovered and interpreted. This heritage raises archaeological and (palaeo-) environmental questions, to which scientists are currently trying to respond by means of Earth observation (EO) techniques (e.g. Lefort et al.,

2004; Lambers and Sauerbier, 2006; Ruescas et al., 2009; Braun, 2010). The latter, in most cases, are used complementarily to conventional and *in situ* investigations (e.g. Lasaponara et al., 2011; Richter et al., 2011). Among others, we mention here the activities being carried out by the Italian mission of heritage Conservation and Archaeogeophysics (ITACA), directly involving the researchers from the Institutes for Archaeological and Monumental Heritage (IBAM), and Methodologies for Environmental Analysis (IMAA) of the National Research Council (CNR) of Italy. A comprehensive review of this mission has been depicted recently by Masini et al. (2012) who discuss the main outcomes achieved from 2007 to date over the region of Nasca.

\* Correspondence to: D. Tapete, Institute for the Conservation and Valorization of Cultural Heritage, National Research Council, Via Madonna del Piano 10, I-50019 Sesto Fiorentino, Florence, Italy.  
Email: deodato.tapete@gmail.com

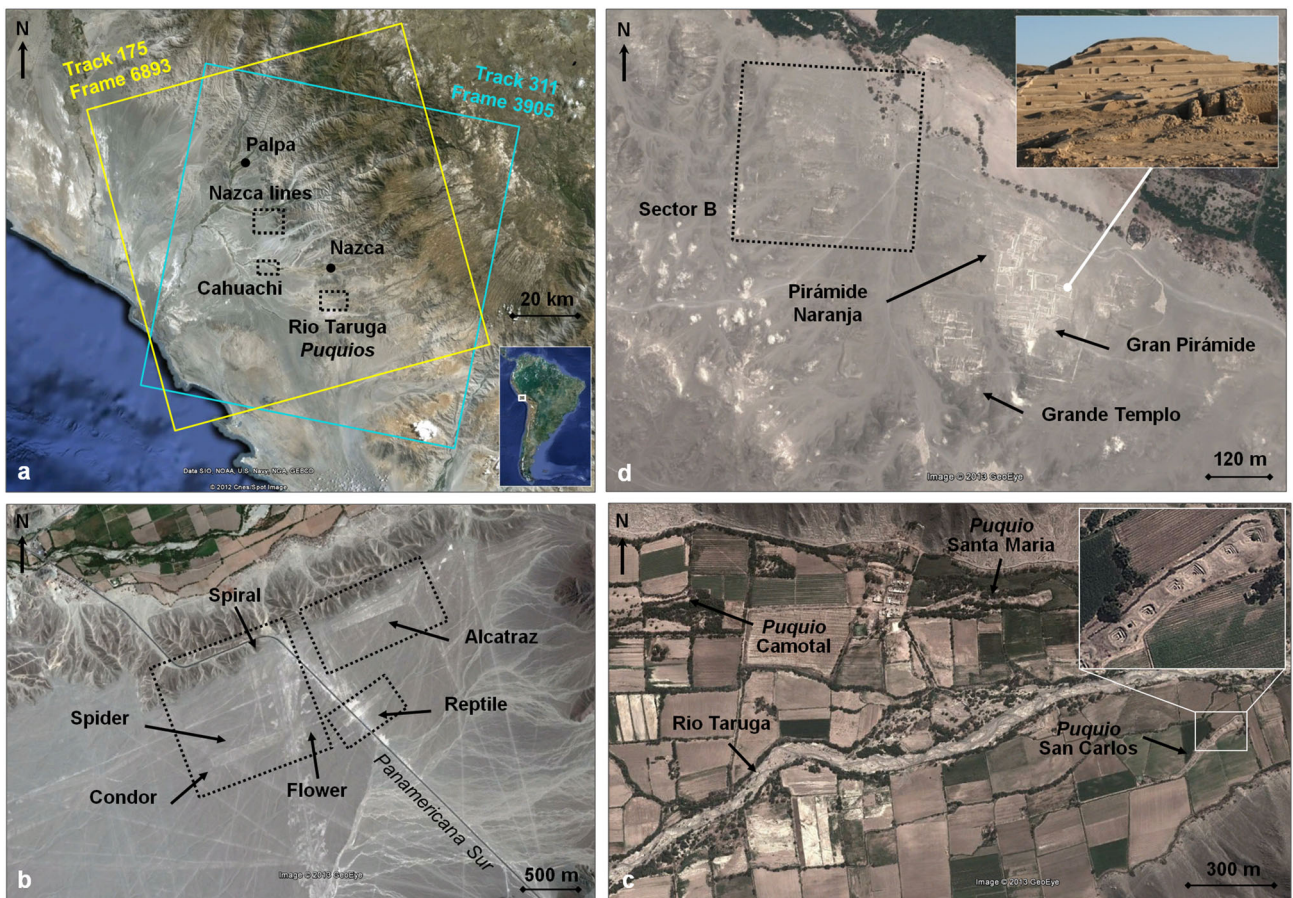


Figure 1. Location and places of interest of the Nasca region, in southern Peru. (Google earth, Image © 2013 GeoEye). (a) footprint of the ENVISAT ASAR IS2 scenes in ascending (Track 175, Frame 6893) and descending (Track 311, Frame 3905) modes available from the European Space Agency's image archives. (b) Nazca Lines close to the Panamericana Sur. (c) Puquios in Rio Taruga floodplain. (d) The Ceremonial Centre of Cahuachi.

There are several elements of archaeological interest linked to the Nasca Civilization. New insights are progressively being added on the religious functions and the history of use and abandonment of the adobe Ceremonial Centre of Cahuachi (Silverman, 1993; Orefici, 2009, 2012; Figure 1d). Very high resolution (VHR) satellite imagery from QuickBird-2, WorldView-1/2 and GeoEye were combined with geomagnetic and ground-penetrating radar (GPR) surveys and contributed to the selection of which sectors to excavate in the area of the Pirámide Naranja (Lasaponara *et al.*, 2011) and more recently in the Templo Sur, where excavations are in progress. Moreover, the recognition of patterns within aerial and satellite imagery and infrared thermograms was also exploited to detect anomalies attributable to the presence of a buried settlement in agricultural areas within the Nazca riverbed (Masini *et al.*, 2012) and infer a potential relationship with the Ceremonial Centre of Cahuachi. These results confirm further that a key to understanding the historical

evolution of the Nasca Civilization relies on a clear and complete knowledge of the spatial distribution of the archaeological findings throughout the whole region.

In this case, searching for archaeological traces to unearth also means to recover the former hydraulic infrastructure. It is well known that ancient inhabitants of the Nasca River valley made such an arid region flourishing thanks to an ingenious system of water collection and storage through the so-called '*puquios*' (Schreiber and Rojas, 2006; Figure 1c). Lasaponara and Masini (2012) recently shed new light on the current hydraulic regime of some *puquios*, by analysing Landsat MSS and TM/ETM+ and Advanced Spaceborne Thermal Emission and Reflection Radiometer (ASTER) data. Such types of information also evidently have relevant implications in the framework of a wider environmental assessment over the whole drainage basin of the Rio Grande (cf. Cigna *et al.*, 2013) and to recover these networks for water supply to local communities.

For purposes of site conservation, we account not only for the authorized activities of archaeological excavations and site promotion, but also for the anthropogenic phenomenon of looting. Such an illegal and destructive action can be controlled with EO-based periodic monitoring, such as that tested by Lasaponara *et al.* (2012) by means of time series of panchromatic and multispectral VHR optical imagery.

With the perspective of a complementary use to the interpretation of EO optical imagery, present research is exploring the usefulness of synthetic aperture radar (SAR) data for recognition of archaeological features and monitoring of cultural heritage. Such data have enormous potential, mainly thanks to the wide availability of long image archives acquired by the ERS-1/2 and ENVISAT satellites of the European Space Agency (ESA) over the past 20 years, with a high level of temporal and spatial coverage over the Earth's surface. Several applications have been carried out recently on the use of SAR amplitude and polarization for archaeological purposes (e.g. Evans and Farr, 2007; Patruno *et al.*, 2012), while SAR phase information is currently largely utilized for site condition monitoring (e.g. Tapete and Cigna, 2012; Cigna *et al.*, 2012; Tapete *et al.*, 2012, 2013). Nevertheless, the advantages of exploiting amplitude information for archaeological prospection need to be investigated still further.

In this regard, interferometric coherence from ERS-1/2 and ENVISAT imagery was used previously over the Nasca region by Lefort *et al.* (2004) and Ruescas *et al.* (2009), who obtained interesting results for surface change detection. Notwithstanding, these methods show limits over vegetated areas, while amplitude-based approaches allow the radar backscattering properties of the scene to be detected and monitored under any condition and land-use, provided that the ground is visible to the satellite sensor.

By applying the SAR amplitude-based method illustrated by Cigna *et al.* (2013), we initiated a set of tests on ESA's C-band SAR archives over Nasca. The first results from ENVISAT advanced synthetic aperture radar (ASAR) 2003–2005 scenes along both descending and ascending orbits are discussed in this paper. Multitemporal and spatial analysis of radar signatures from archaeological features belonging to the Nazca Lines and the adobe structures in Cahuachi is preparatory to perform tests of archaeological prospection and monitoring of both the archaeological structures and the ancient network of *puquios*.

This research is part of an ongoing joint project between the British Geological Survey (BGS) of the Natural Environment Research Council (NERC) in the UK, the Institute for the Conservation and

Valorization of Cultural Heritage (ICVBC-CNR), IBAM-CNR and IMAA-CNR, and is supported by ESA through the provision of ASAR imagery via the Category-1 Project Id.11073.

## Archaeological heritage of the Nasca region

Based on the SAR processing performed over the entire drainage basin of the Rio Grande (cf. the environmental assessment discussed by Cigna *et al.*, 2013), archaeological prospection and monitoring at the local scale were undertaken on three main areas of cultural interest:

- (i) The Nazca Lines with stylized geoglyphs depicting the famous Spider, Flower and Spiral (hereinafter Group 1) and Alcatraz (Group 2), which are located west and east of the road Panamericana Sur respectively (Figure 1b);
- (ii) The *puquios* Santa María, San Carlos and Camotal in the floodplain of Rio Taruga (Figure 1c);
- (iii) The archaeological site of Cahuachi (Figure 1d).

The most famous archaeological heritage of the region is undoubtedly the geoglyphs referred to as the 'Nazca Lines', inscribed on the World Heritage List of UNESCO in 1994. These drawings are characterized by a combination of geometric and biomorphic motifs, and are thought to be sacred pathways. They were scratched on the ground surface by removing the dark gravels of the valley and exposing the underlying unpatinated and lighter coloured ground (i.e. 'negative geoglyphs') (Reinhard, 1996; Orefici, 2012). Sources of potential damage for the Nazca Lines can be of human origin and, secondarily, from natural phenomena, e.g. due to exceptional events of *huaycos*, which are huge streams of viscous muddy water. Damage from run-off and surface flowing water should not be of particular concern, in light of the limited amount of precipitation per year recorded for the region (average 10 mm/yr, as expected for a sub-tropical desert; cf. ONERN, 1971).

The Nazca Lines therefore can be assumed as reference targets to estimate the effects of the surface roughness with regard to the radar wavelength (e.g. Braun, 2010). On the other hand, the identification of backscattering coefficient attributable to certain materials and surface roughness can be used to recognize patterns due to the presence of geoglyphs, and/or to enhance morphological or compositional changes. This analysis might be utilized as an indicator of the condition of the geoglyphs and other archaeological features that are vulnerable to surface processes and hazards.

Among the latter we also consider the ancient waterways and sources of irrigation water constituted by the *puquios*, i.e. aqueducts in the form of horizontal water wells, open trenches and/or underground galleries, which were crucial for such an arid region to favour the development of a social organization and survival strategies (Figure 1c). Parts of them are still active whereas other parts are abandoned, such as the *puquio* Camotal, located north of Rio Taruga and approximately 1 km west and 2 km northwest from the still functioning *puquios* Santa María and San Carlos, respectively. The latter are trench and filled-trench gallery type *puquios* and are characterized by large conical openings called '*ojos*' (i.e. 'eyes' in Spanish), which are visible at the ground level and allow access into the subterranean galleries (see the inset in Figure 1c; cf. Figure 7i). The preservation of the ancient *puquios* is essentially linked to the availability of a comprehensive inventory, as well as to the possibility of monitoring seasonal variations in their hydraulic regime to understand whether hazards from droughts and climate change can have impacts on their functionality and maintenance.

In Cahuachi, natural and human hazards are real issues for the still buried archaeological heritage and those already unearthed. Located on a large barren area on the left side of the Rio Nazca (Figure 1d), the Ceremonial Centre of Cahuachi contains around 40 archaeological mounds, which have been progressively excavated since 1984 by the Italian–Peruvian Mission directed by G. Orefici. Up to the present the major archaeological structures brought to light are concentrated within a 0.16 km<sup>2</sup> area considered by the archaeologists as the monumental core of Cahuachi; and this includes the Gran Pirámide, Grande Templo and part of Pirámide Naranja (Figure 1d). These three structures are made of adobe and have a history spanning from 400–100 BC to AD 400–450 (Silverman, 1993; Orefici, 2012). They show the superimposition of different building phases, which are testified by walls, filled-in platforms and terraces, and underwent remarkable transformations (Orefici, 2009; Masini *et al.*, 2012) that occurred until their final abandonment, also due to damage produced by severe mudslides and earthquakes. Systematic archaeological excavations have been undertaken in this area over recent years, including the southern side of the Gran Pirámide and some sectors of the Templo del Escalonado and Pirámide Naranja, in 2003–2005 (Masini *et al.*, 2012). Parallel restoration and reconstruction activities were also undertaken (cf. Figure 9).

A further area of archaeological interest is the so-called Sector B, located northwest of Cahuachi (Figure 1d). This sector covers an area of ~0.10 km<sup>2</sup>, and includes a

U-shaped courtyard enclosing several archaeological mounds still to be excavated, but in many cases already affected by looting. Incidence of this illegal activity in the Nasca region and the actual potentials of remote sensing to support its monitoring and even its prevention, have been demonstrated and discussed recently by Lasaponara *et al.* (2012). In that study, the authors employed change detection with LISA (local indicator of spatial autocorrelation; see Anselin, 1995) processing of VHR satellite imagery and identified the intensification of looting in 2002–2008 by estimating the increasing number of pits within an area between the southeastern corner of Sector B and the archaeological excavations in the Pirámide Naranja and Gran Pirámide.

In this cultural and dynamic context, we tested SAR-based change detection to detect surface modifications potentially attributable to human activities, as well as to natural land surface processes.

## ENVISAT ASAR processing

Eight ENVISAT ASAR IS2 images acquired along a descending orbit between 04 February 2003 and 15 November 2005, and five images in the corresponding ascending mode between 24 July 2005 and 11 November 2007 from ESA's archives were exploited to investigate the archaeological heritage of the Nasca region (Figure 1a).

Both stacks, characterized by a swath of 105 km, VV polarization, and line of sight (LOS) look angle of 22.8° (referred to the centre of the scene), are acquired by a C-band spaceborne radar sensor operating with a wavelength ( $\lambda$ ) of 5.6 cm (i.e. frequency of 5.33 GHz), a nominal repeat cycle of 35 days, and orbit inclination (or track angle) of 12.9° at the latitudes of Nasca. The nominal ground range resolution of ~30 m allows these SAR data to be classified as medium resolution imagery.

Data processing was carried out following the method described by Cigna *et al.* (2013), to which the reader should refer for full details. Figure 2 summarizes the main steps of the methodology to generate the geocoded derived products, which were used directly in the present research for archaeological prospection and monitoring.

Focusing of the ENVISAT ASAR Level 0 (raw data) products to single look complex (SLC; i.e. amplitude and phase; Figure 2) was performed through the range-Doppler processing sequence, by using the GAMMA SAR and Interferometry Software (GAMMA, 2012) and ASAR auxiliary data provided by ESA (i.e. external characterization files and instrument characterization files).

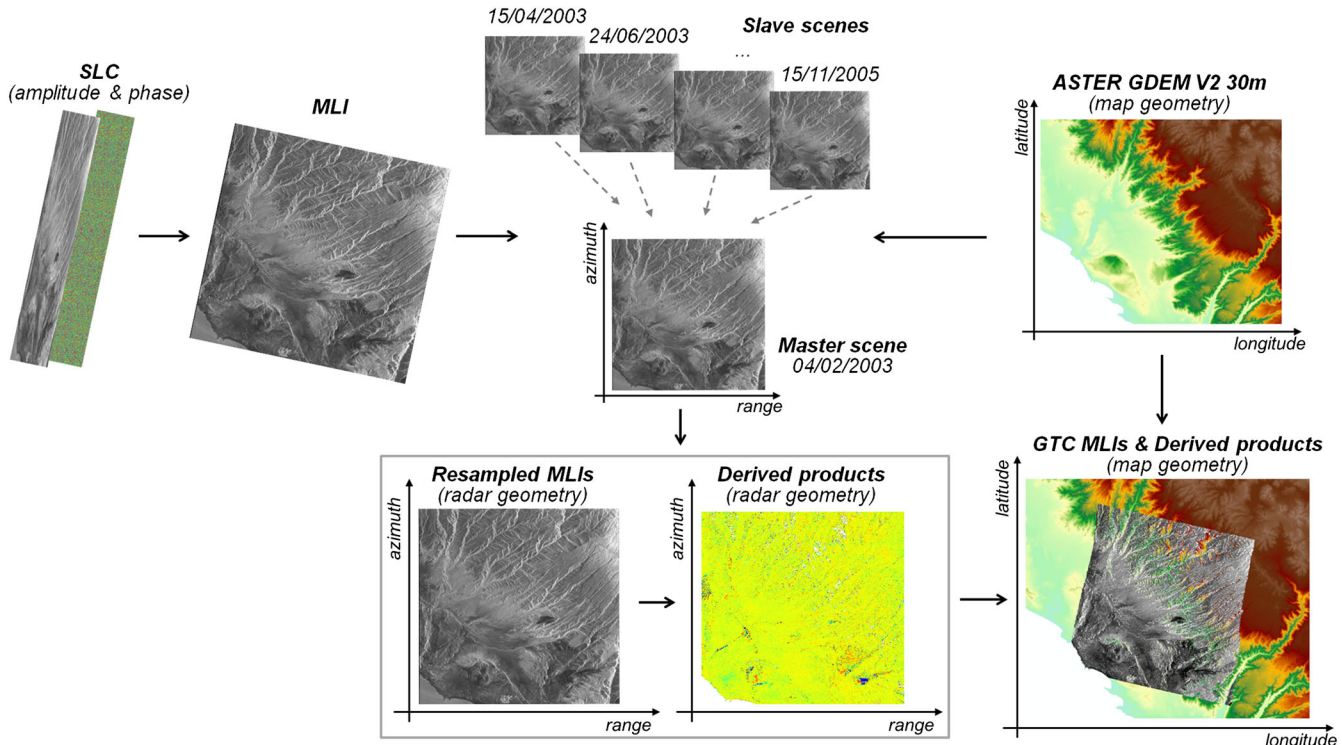


Figure 2. Methodology employed for the ENVISAT ASAR image processing and generation of geocoded derived products. SLC, single look complex; MLI, multilook intensity; GTC, geocoded terrain corrected. This figure is available in colour online at [wileyonlinelibrary.com/journal/arp](http://wileyonlinelibrary.com/journal/arp)

The second step consisted in the generation of multilook intensity (MLI) images in slant range–Doppler coordinates from the amplitude component of the SLC data (Figure 2). A multilook factor of five in azimuth was chosen to reduce the effects of radar speckle, with consequent decrease of the azimuth pixel spacing and resolution up to  $\sim 20.5$  m and  $\sim 22.7$  m respectively.

The intensity values of the SLCs were computed as radar backscattering coefficient  $\sigma^0$  (sigma nought), and then converted to dB. The coefficient  $\sigma^0$  quantitatively expresses the radar signal backscattered to the sensor, normalized (at least to a first approximation) to the horizontal ground surface and referred to as per unit area on the ground. On equal wavelength and polarization of the radar signal (which are related to the spaceborne radar sensor and its acquisition mode),  $\sigma^0$  depends on the properties of the scattering material, and in particular on its dielectric constant, roughness and orientation. This relationship is essential for the purpose of using amplitude information to detect, map and monitor surface characteristics that can be referred to archaeological structures and cultural features.

The key step of the processing was the precise co-registration of the ASAR scenes to a single master (i.e. 04 February 2003 for the descending stack), the

generation of the derived products and subsequent geocoding, to move from the radar geometry (slant range, azimuth) to the map geometry (WGS84 latitude/longitude) (Figure 2). For these purposes, we used the 30-m ASTER global digital elevation model (GDEM) V2 released by US National Aeronautics and Space Administration and Ministry of Economy, Trade, and Industry (Japan) (ASTER GDEM Validation Team, 2011) rather than the 90-m resolution SRTM (Shuttle Radar Topography Mission) V4. An accurate analysis of the SRTM revealed significant artefacts over the mountainous areas around the valleys of Nasca (cf. Figure 3).

The precise geocoding of the co-registered MLIs and all derived products to the WGS84 datum allowed the combination of the radar products with external layers and ancillary geospatial layers, such as ASTER multispectral data.

The following four products were derived from the co-registered MLIs:

- (i) temporally averaged radar signatures of the observed area, i.e. the average backscattering coefficient ( $\bar{\sigma}_i^0$ ) of each pixel within the scene over the monitoring time ( $t$ ) based on the total number of the processed scenes ( $n$ );

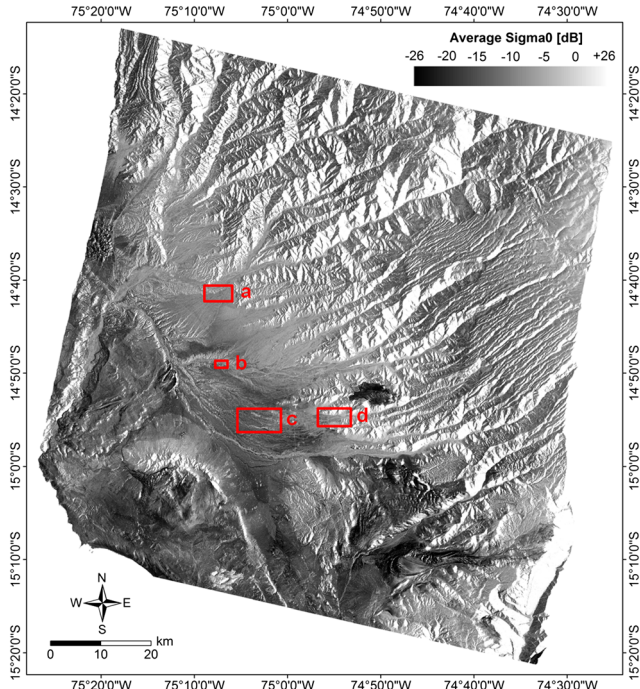


Figure 3. Average ASAR MLI in descending mode in 2003–2005 over the Nasca region: (a) Nazca Lines; (b) Cahuachi; (c) Rio Taruga; and (d) Puquios.

- (ii) time series of spatially averaged radar signatures for selected areas of interest (AOIs), i.e. the graphs showing the temporal variation of the backscattering coefficient calculated as the average value of the  $N$  pixels within each AOI [ $\sigma_{AOI}^0(t)$ ];
- (iii) image ratios ( $R_{\sigma^0}$ ) of different pairs of spatially filtered MLIs, which enhance the  $\sigma^0$  changes occurring over the scene during the time interval between the two MLIs;
- (iv) RGB (red-green-blue) or RC (red-cyan) colour composites of three or two MLIs respectively, where those pixels with constant radar backscattering are shown with grey levels, while those that changed are highlighted with colours of tint corresponding with the scenes recording higher  $\sigma^0$ .

Three ASTER multispectral scenes acquired on 30 May 2003, 1 June 2004 and 10 June 2007 in the visible near-infrared (VNIR), shortwave infrared (SWIR), and thermal infrared bands (TIR), with spatial resolutions of 15, 30 and 90 m respectively, were used to complement the radar products. Normalized difference vegetation index (NDVI) and water index (NDWI) maps obtained from the red, NIR and SWIR bands of the ASTER scenes were also useful to cross-validate vegetation and soil moisture changes that occurred in the period 2003–2007.

## Radar imaging of the Nazca Lines and Cahuachi in 2003–2005

Both the descending and ascending data stacks were processed over the entire region of Nasca. Figure 3 shows the average ASAR MLI in descending mode for the period February 2003 to November 2005.

Trapezoidal geoglyphs belonging to Groups 1 and 2 of the Nazca Lines near the Panamericana Sur (cf. Figure 1b; Figure 4a), as well as anthropogenic (infra)structures, such as the motorways, are easily recognizable, provided that their size is greater than the ground resolution of the processed SAR imagery (i.e. ~30 m for ENVISAT ASAR IS2 data). The trapezoidal geoglyphs associated with Groups 1 and 2 have, indeed, a length of a few hundreds of metres and width of tens of metres.

In particular, WSW–ENE oriented darker features in the average MLI correspond to the trapezoids close to the Flower and Alcatraz (Figure 4b). The darker appearance of the latter is due to their typical ‘construction technique’ (see the above mentioned categories of Nasca geoglyphs) and clearly marks the trapezoids with respect to the surrounding bare soil. Less visible, but still appreciable, is the trapezoid associated with the geoglyph representing a lizard (‘Reptile’), which was unfortunately cut during the building of the Panamericana Sur (Figure 4b).

Conversely, geoglyphs with smaller dimension than the average resolution of the processed images (e.g. Flower, Spiral and Spider; see Figure 4d and e) are not clearly visualized, as suggested by the comparison with the corresponding ASTER 3 N-2-1 image (Figure 4a and b) and/or other optical satellite imagery and aerial photographs (cf. Figure 1b).

The signature-based recognition of classes of elements on the ground was preparatory to the extraction of the times series of  $\sigma_{AOI}^0(t)$  in 2003–2005, i.e. the trends of  $\sigma^0$  for each AOI throughout the monitoring period 2003–2005. Such diagrams were helpful to assess whether an AOI changed its backscattering properties over time or not.

In Figure 4c the time series of the two trapezoids belonging to the geoglyphs Groups 1 (Spider, Flower and Spiral) and 2 (Alcatraz) are compared (see details of Group 1 depicting the spider and part of the trapezoid, and the flower in Figure 4d and e). Each estimate in the graph shows the average value of  $\sigma^0$  and related spatial standard deviation at the date of image acquisition. The standard deviation expresses the spatial variability of the  $\sigma^0$  values within a certain AOI at the acquisition time considered. Besides the difference in the absolute value of each estimate, the two time series share a similar trend (Figure 4c). The relatively low

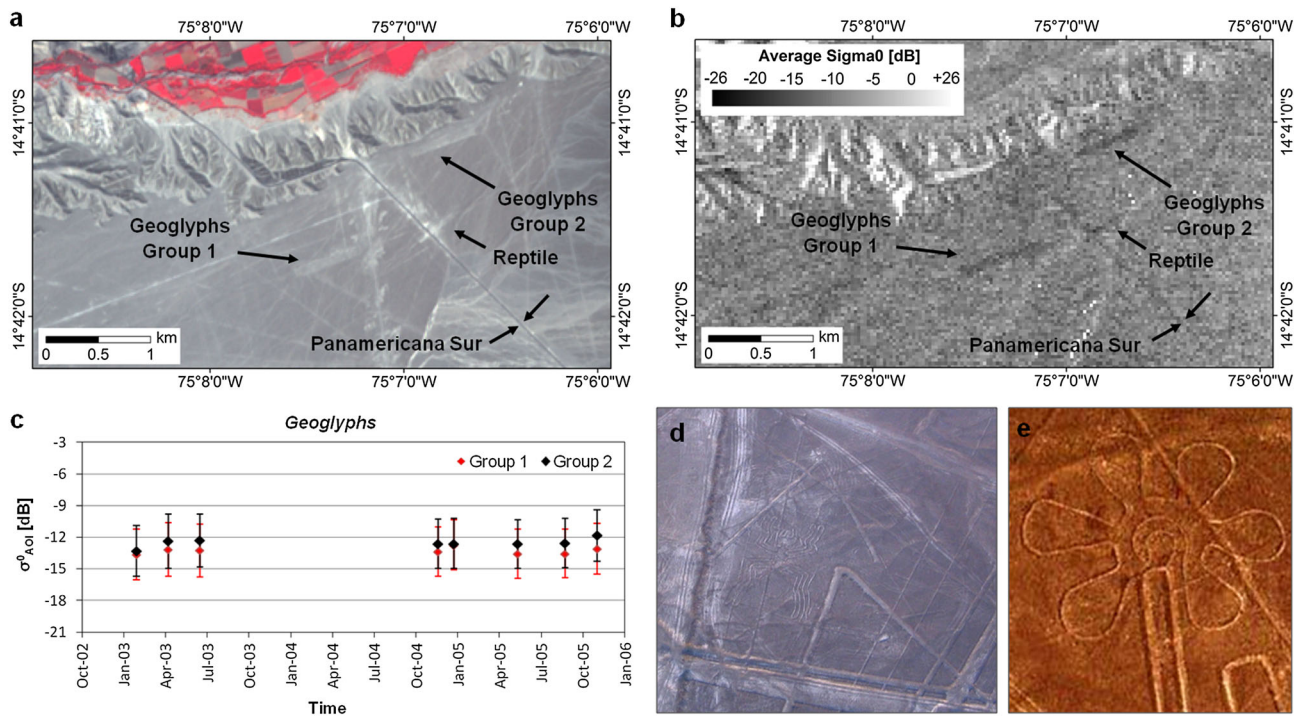


Figure 4. Area of the Nazca Lines. (a) RGB colour composite of bands 3N-2-1 of an ASTER scene acquired on 30 May 2003 [3N, NIR (nadir looking) at 0.76–0.86  $\mu\text{m}$ ; band 2, red at 0.63–0.69  $\mu\text{m}$ ; band 1, green/yellow at 0.52–0.60  $\mu\text{m}$ ]. (b) Average ASAR MLI in descending mode in 2003–2005. (c) Temporal series of radar backscattering coefficient in 2003–2005 for the two trapezoids of the Nazca geoglyphs Groups 1 and 2. Details of (d) the spider and one of the trapezoids, and (e) the flower located within Group 1.

standard deviation (i.e. ~2.2–2.4 dB) is probably due to the spatial homogeneity of the surface of the two trapezoids, which is clearly visible in the average MLI (cf. Figure 4b), and the small size of the AOI considered (only ~0.1  $\text{km}^2$  each). Both series also suggest that no major variations or univocally definable trends (neither increase nor decrease of  $\sigma^0$  values) occurred in 2003–2005.

Moving to the archaeological site of Cahuachi (Figure 5a), it is worth comparing the different radar signatures retrieved in the average ASAR MLIs that were generated by using the ascending scenes in July 2005 to November 2007 and the descending images in February 2003 to November 2005. The ascending geometry (Figure 5b) highlights the morphological and topographic features surrounding the Grande Templo, within the monumental core of Cahuachi. Emerging from the darker areas corresponding with the bare soil and platforms, the two lighter bands are probably due to signal foreshortening affecting west-facing slopes. On the other hand, the descending MLIs better reveal the backscattering of the platforms and adobe structures of the Gran Pirámide, and Pirámide Naranja, while the sloping surfaces enclosing the Grande Templo appear dark (Figure 5c).

This example demonstrates the role played by the satellite acquisition geometry and its spatial relationship with the orientation, inclination and shape of the backscattering surfaces on the ground (besides the material properties, composition and moisture content).

The time series extracted from the descending MLIs for the area of the Pirámide Naranja and one of the archaeological mounds located within Sector B (cf. Figure 1d) show similar  $\sigma^0_{AOI}(t)$  trends, without relevant temporal changes (Figure 5d). Although both AOIs are characterized by relatively small extent (~0.02  $\text{km}^2$ , i.e. only 20–25 pixels), the relatively high standard deviation (i.e. ~3.5–4.5 dB) for a single measure of both the time series is justifiable due to the non-homogeneity of the two AOIs, which evidently include surfaces characterized by different backscattering properties.

## Recognition of *puquios* and water-level changes in 2003–2005

As previously mentioned, further archaeological heritage of the Nasca region is represented by the Ancient

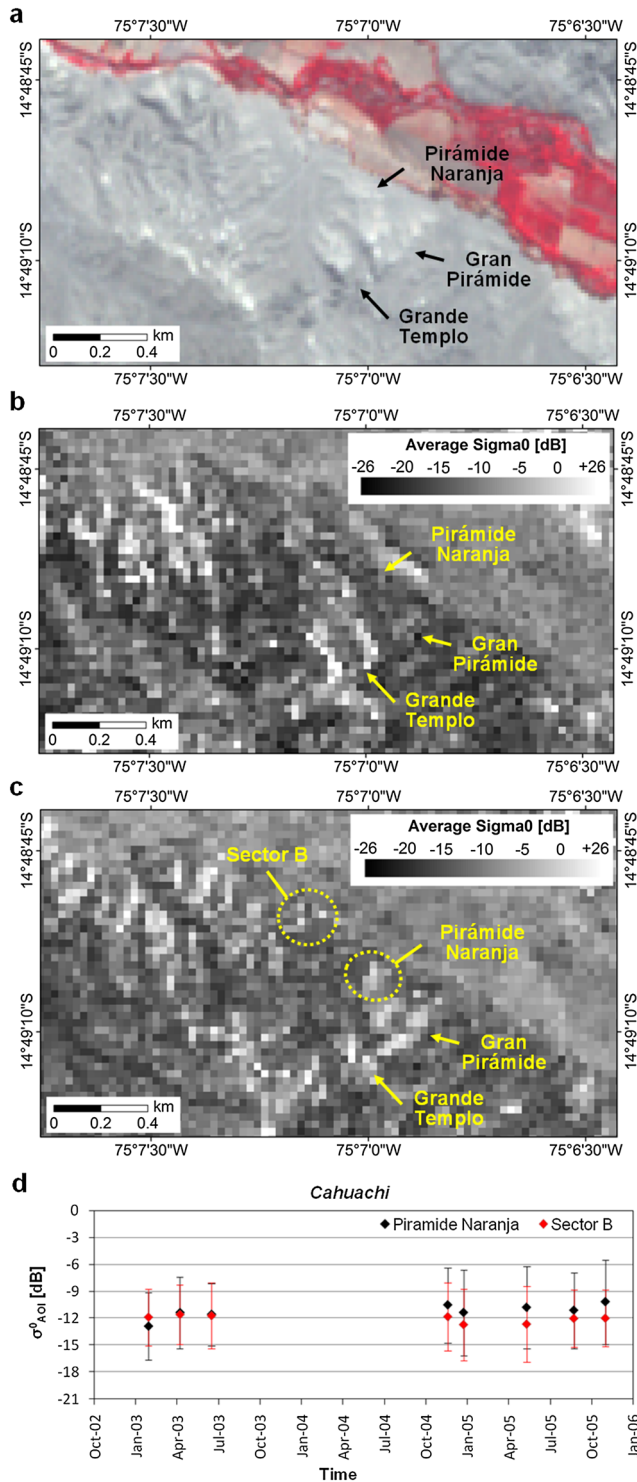


Figure 5. Area of Cahuachi. (a) RGB colour composite of bands 3N-2-1 of an ASTER scene acquired on 30 May 2003 [3N, NIR (nadir looking) at 0.76–0.86 µm; band 2, red at 0.63–0.69 µm; band 1, green/yellow at 0.52–0.60 µm]. (b) Average ASAR MLI in ascending mode in 2005–2007. (c) Average ASAR MLI in descending mode in 2003–2005. (d) Temporal series of radar backscattering coefficient in 2003–2005 for a mound within Sector B and the area of the Pirámide Naranja.

Nasca *puquios* and the palaeoenvironmental features, which are still preserved in the Nasca landscape and can be detected and investigated by means of remote sensing techniques. Such heritage studies can find mutual benefits from environmental assessment of the hydraulic regime of the present rivers, based on the identification of surface indicators that can be correlated with buried cultural features. For instance, monitoring of agricultural/vegetated areas can be very helpful, because crops tend to adapt to water availability and its fluctuations over time, thereby changing very rapidly, and they act as a reliable indicator of the presence of groundwater.

With this perspective, we performed RC colour composites of pairs of MLIs for change detection purposes over the fluvial areas that were previously analysed by Lasaponara and Masini (2012), in particular over a large dry hydrographic reticulum lying within the desert between the Rio Nazca and the Pampa de Chauchilla, characterized by the presence of underground rivers. The latter often show an intermittent water flow due to soil infiltration capacity, which causes the disappearance of parts of the river courses under the ground level.

Figure 6a reports the results of RC colour composite of two MLIs acquired on 30 November 2004 and 15 November 2005 respectively. Cyan coloured areas are those backscattering more in November 2005 than 2004, probably due to an increase of soil moisture during 2005. In contrast, the red coloured areas indicate a decrease of radar backscattering from 2004 to 2005, thereby suggesting a decrease of soil moisture and/or vegetation.

The area identified as V3 (yellow dashed square in Figure 6a) corresponds with a sector of the tributary Rio Taruga where water flows in the wet season. Over this sector the multitemporal comparison of the ASTER-derived 2003, 2004 and 2007 NDVI and NDWI by Lasaponara and Masini (2012) clearly detected some changes occurring over time as reliable indicators of groundwater level fluctuations (Figure 6b). The same authors classified the hydraulic regime of this sector of the stream as ephemeral (intermittent), due to the spatial and temporal variability of its NDWI values over time, and also identified two disused *puquios* just south of the tributary Taruga, by means of a VHR GeoEye 2011 scene. As of 2011, the most recent was still characterized by the presence of vegetation fed by water that still flowed through it.

These *puquios* are less than 5 m in size, and so are not distinguishable within the ASAR MLIs due to their resolution not being capable of detecting features smaller than ~30 m. Nevertheless, Figure 6a shows a linear cyan feature (see the yellow arrows for a clear recognition) that

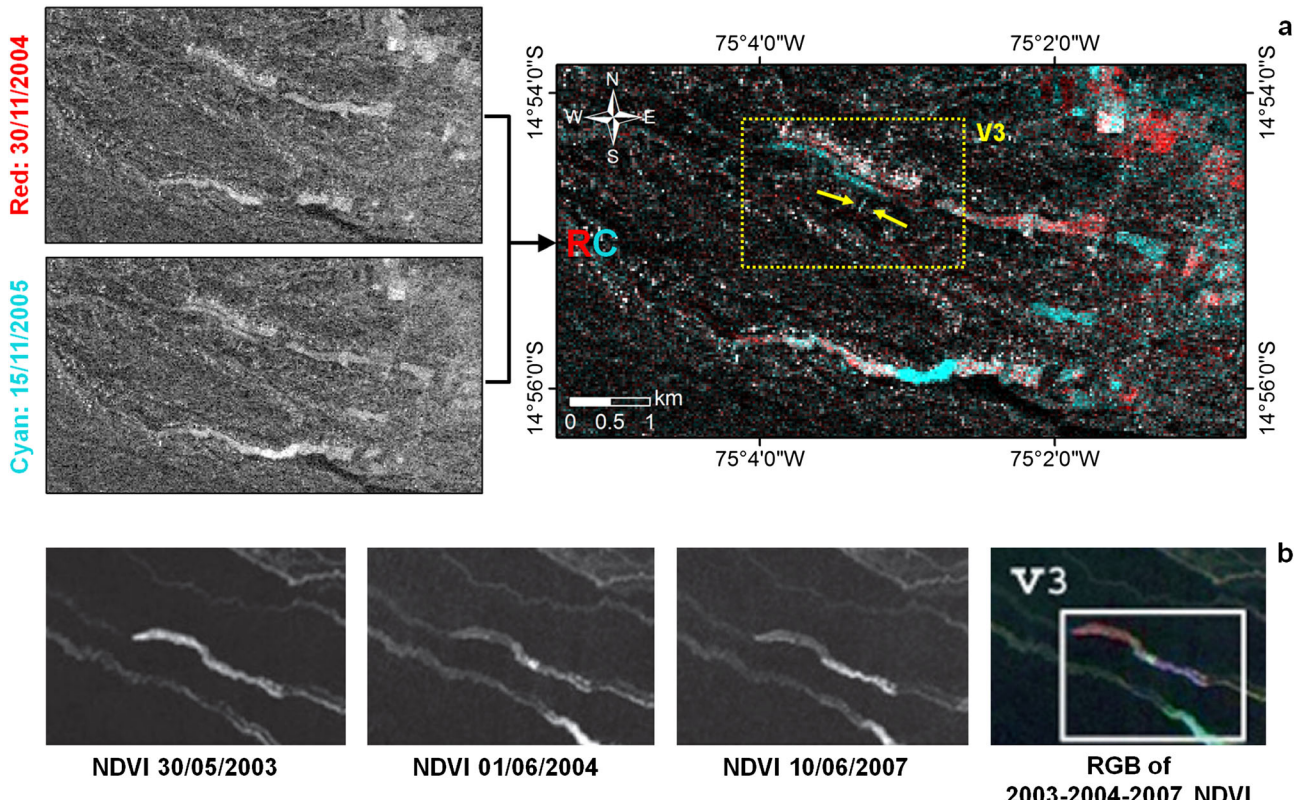


Figure 6. (a) RC colour composite of the ASAR MLIs acquired on 30 November 2004 and 15 November 2005. (b) RGB colour composite of the ASTER-derived NDVI in 2003, 2004 and 2007 from Lasaponara and Masini (2012). The yellow arrows in (a) indicate the location of an ancient *puquio*.

follows the younger *puquio* and may be an indicator of water-level fluctuations between November 2004 and November 2005 beneath it. This outcome, enhanced by the mutual validation between ENVISAT ASAR and ASTER results, is quite encouraging to assess the actual capability for the recognition of cultural features.

By investigating the portion of the Taruga Valley, namely the Taruga Irrigation Sector according to the Peruvian Ministerio de Agricultura (Figure 7a), the average MLI allows the identification of the still functioning *puquios* Santa María (Figure 7i and j) and San Carlos (cf. Figure 1c and the associated inset). The latter can be distinguished more clearly within the average MLI as an effect of the presence of less vegetation and more bare soil, a feature of the surroundings of the *puquio* (Figure 7c). The area of the disused *puquio* Camotal appears darker than the other *puquios*, thereby suggesting different material composition and surface roughness, which are probably due to its abandoned condition.

The track of the two functioning *puquios* is still appreciable in the RGB colour composite of the ASTER

NDVI 2003, 2004 and 2007 (Figure 7b). Conversely, major changes of the backscattering coefficient cannot be detected in either the ASAR RGB colour composite throughout 2003 (Figure 7d), or the RC colour composite 2004–2005 (Figure 7f). The impression that no significant changes occurred over the monitoring period is confirmed by the amplitude change detection maps, in particular within the yearly ratio between November 2004 and November 2005, i.e. comparing corresponding seasons of two consecutive years (Figure 7h). Conversely, it is worth noting that the ratio between May and November 2005 shows a decrease of the backscattering coefficient in the neighbouring vegetated area of the *puquio* Santa María (especially along the southern side of the *puquio*) and in the agricultural fields east of the *puquio* San Carlos (Figure 7g). This evidence can be an indication of variable water flows through the ancient *puquios*, and mutable soil moisture of the surrounding fields. Similar patterns are observed between February 2003 and November 2005 (Figure 7e). The absence of variations over the *puquio* Camotal can be reasonably justified by its condition of disuse.

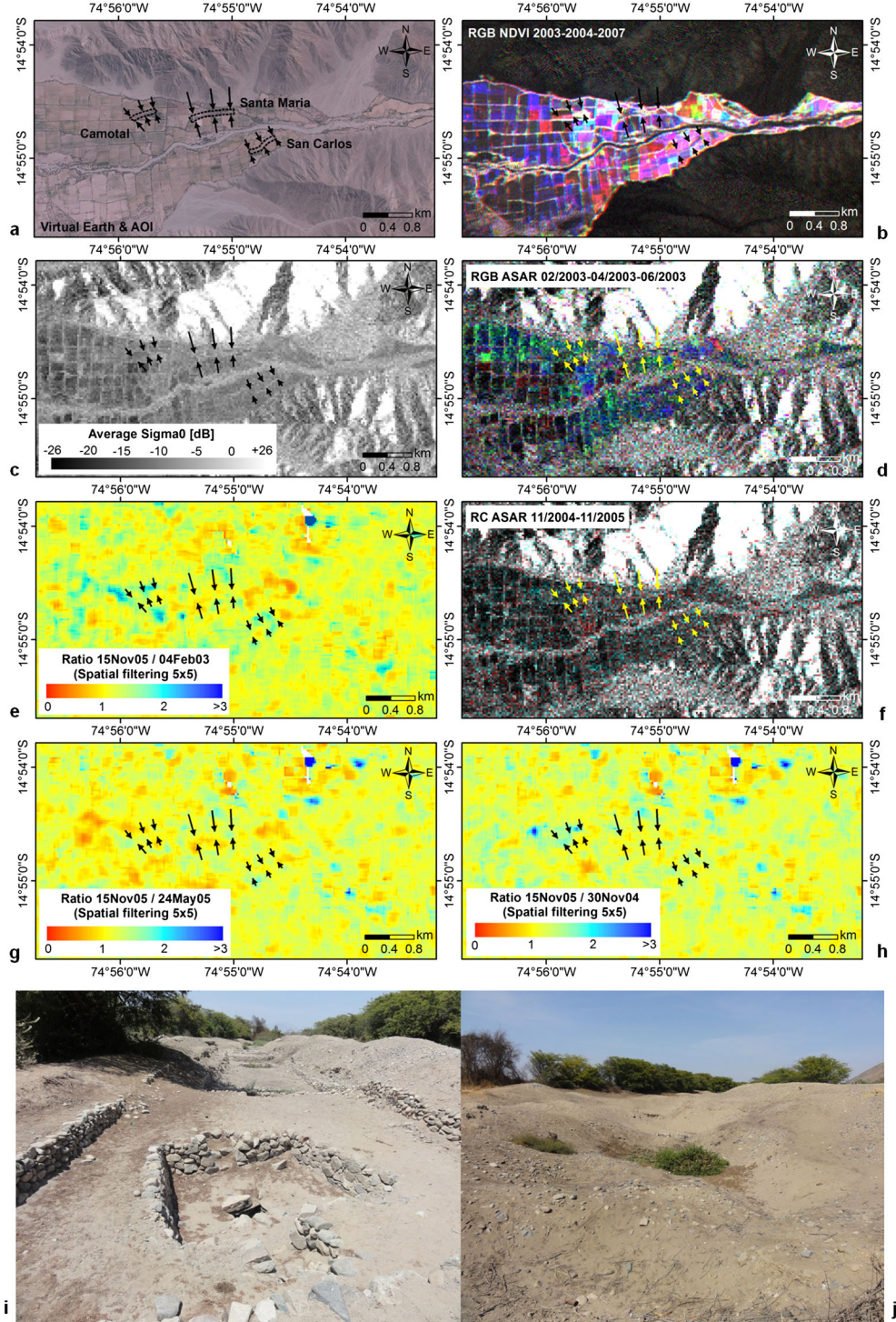


Figure 7. (a) Virtual Earth image of Rio Taruga floodplain with indication (see black arrows) of the still functioning *puccios* of Santa María and San Carlos, and the abandoned *puccio* Camotal. Corresponding views of: (b) RGB colour composite of the ASTER-derived NDVI in 2003, 2004 and 2007; (c) average MLI in descending mode in 2003–2005; (d) RGB colour composite of 04 February 2003, 15 April 2003 and 24 June 2003 ASAR descending scenes; and (f) RC colour composite of the 30 November 2004 and 15 November 2005 scenes. Amplitude change detection maps based on the ratio of the backscattering coefficient between (e) February 2003 and November 2005, (g) May 2005 and November 2005, (h) November 2004 and November 2005. (i–j) Two segments of the *puccio* Santa María: (i) one still functioning, (j) another abandoned. In (i) a detail of a square 'ojito' is shown.

## Monitoring the archaeological site of Cahuachi

Tests of archaeological prospection and site condition monitoring were carried out over Sector A, i.e. the monumental core of the Ceremonial Centre including Grande Templo, Gran Pirámide and Pirámide Naranja, and Sector B, i.e. the area enclosing the archaeological mounds located northwest of Cahuachi (Figure 8a and b).

As expected, the limits in ground resolution ( $\sim 30$  m) do not allow single archaeological features to be detected by means of ENVISAT ASAR imagery, nor surface patterns potentially attributable to the presence of buried structures. Their dimension cannot be resolved at this scale of resolution, as clearly evident from the MLI (Figure 8c) and its comparison with the WorldView-1 panchromatic image acquired on 31 July 2008 with ground sample distance (GSD) of 58.10 cm

(Figure 8b). Despite the temporal averaging of the entire eight-image ASAR descending data stack, speckle is still high and does not allow the different targets on the ground to be distinguished.

On the other hand, the processed descending ENVISAT ASAR scenes were helpful to monitor the  $\sigma^0$  variations in 2003–2005 over both Sectors A and B, through the production of amplitude change detection maps based on pairs of ASAR MLIs, which were spatially filtered by using a 3 by 3 pixel window (Figure 8d–f). The change detection maps were obtained from ratioing between different pairs of scenes, and in particular between the following:

- (i) 24 May 2005 and 15 November 2005, to compare two opposite seasons within the same year of observation and identify the surfaces and anthropogenic structures that may show different conditions (Figure 8d);

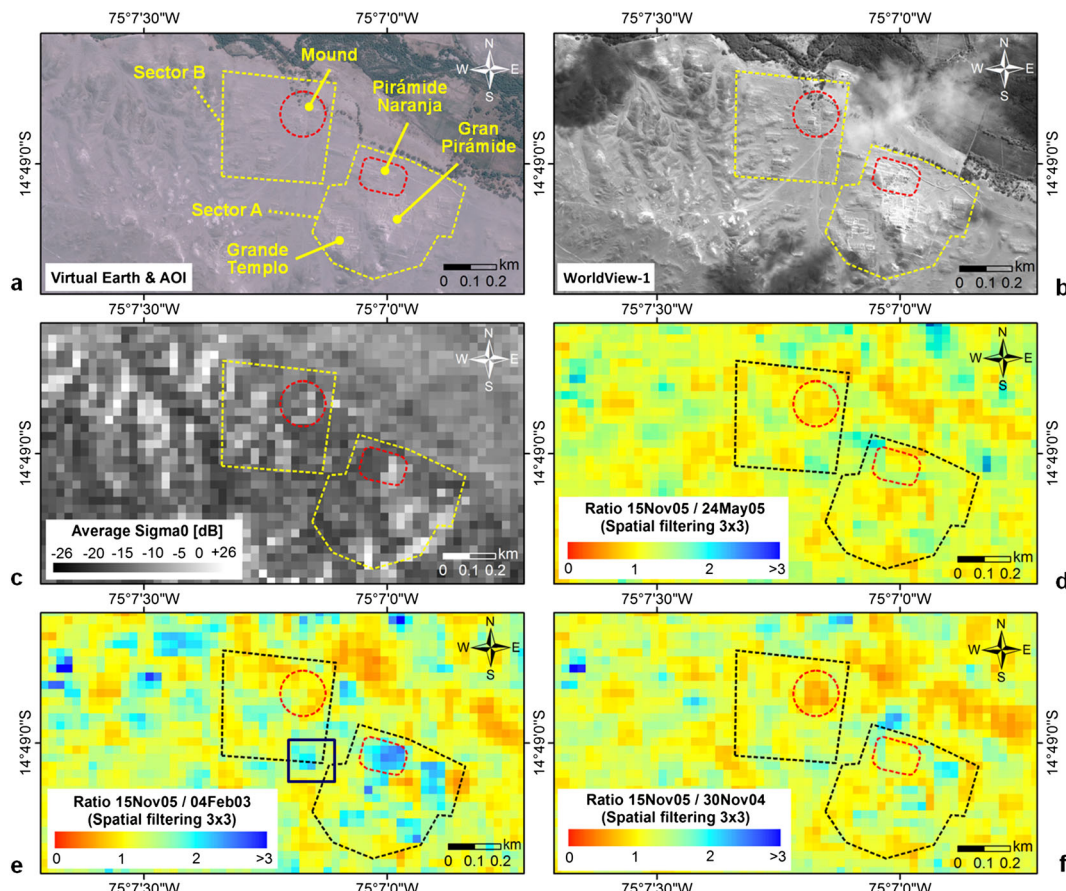


Figure 8. (a) Virtual Earth image of the Ceremonial Centre of Cahuachi (Sector A) and Sector B enclosing archaeological mounds. Corresponding views of: (b) 2008 WorldView-1 panchromatic image (©DigitalGlobe, Inc., All Rights Reserved); and (c) average MLI in descending mode in 2003–2005. Amplitude change detection maps based on the ratio of the backscattering coefficient between (d) May 2005 and November 2005, (e) February 2003 and November 2005, (f) November 2004 and November 2005. The red circle and rectangle indicate the archaeological mound within Sector B and the excavated sector of Cahuachi, respectively, which show interesting change patterns in the period monitored. The black square over the southeast corner of Sector B in (e) corresponds with the area of looting studied by Lasaponara *et al.* (2012).

- (ii) 04 February 2003 and 15 November 2005, to analyse the changes that occurred throughout the entire monitoring period, from the first to the last available acquisition of the descending stack, to image the evolution of Cahuachi, especially in relation to archaeological excavations and information regarding the recent conservation history (Figure 8e);
- (iii) 30 November 2004 and 15 November 2005, to finally discover any changes occurring between two corresponding seasons of consecutive years (Figure 8f).

The comparison between the amplitude change detection maps for the ASAR pairs (i) and (iii) enhances a decrease of the backscattering coefficient over the northeastern part of Sector B, within an area corresponding with mound number 6 (cf. Masini *et al.*, 2012; Figure 8d and f). A clear orange-coloured pattern indicating a decrease of the radar backscattering can be identified in the change detection map November 2004 and November 2005 (Figure 8f), thereby suggesting significant alteration of local surface properties in the last year monitored. As the two compared scenes date to the

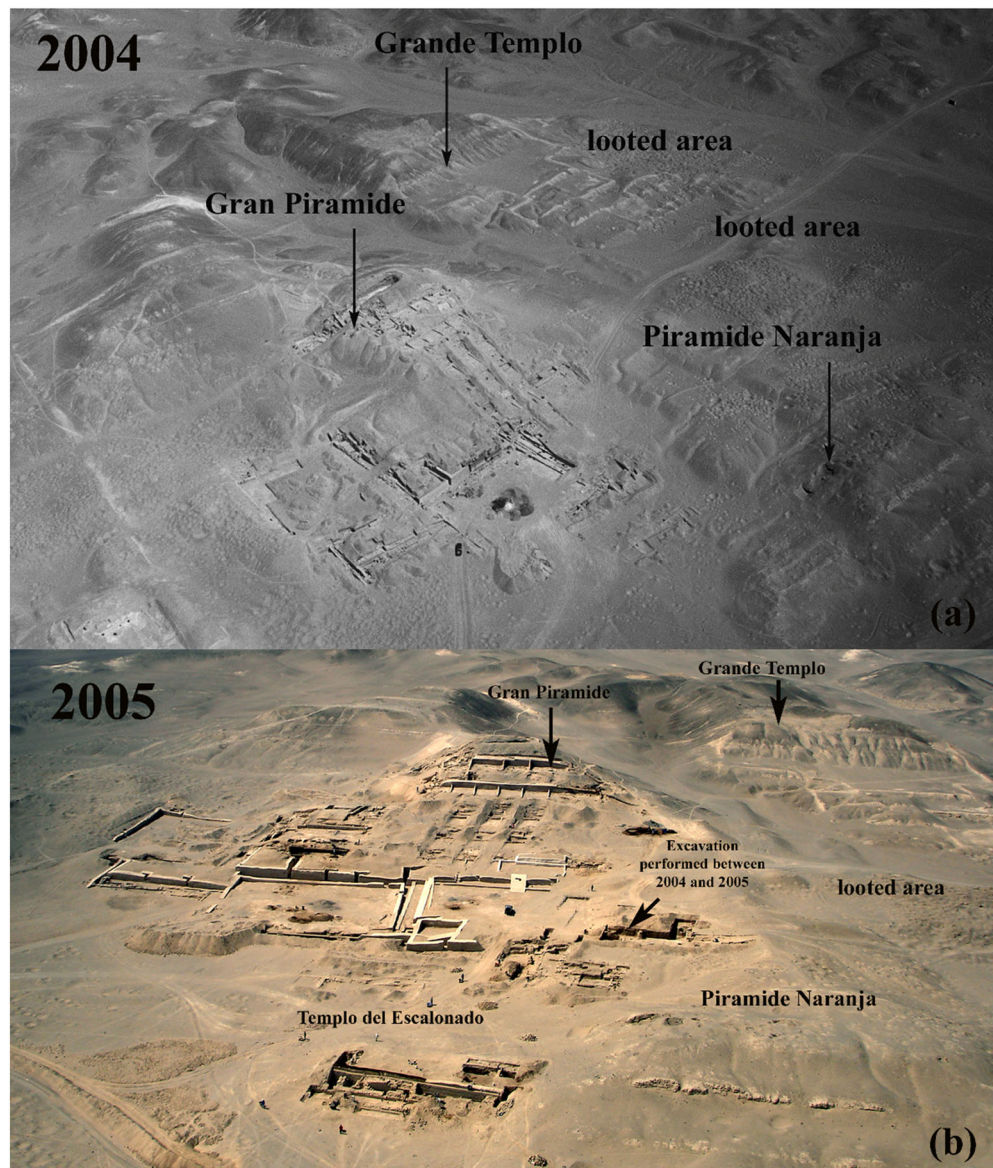


Figure 9. (a) Aerial photograph taken in 2004 of the core of Cahuachi, including the Gran Pirámide, Grande Templo, Pirámide Naranja and two areas strongly affected by looting (courtesy of G. Orefici). (b) The same part of Cahuachi taken from a different view in 2005 (courtesy of G. Orefici). An excavated sector of the Pirámide Naranja is shown, which confirms the high ratio of the backscattering coefficient between February 2003 and November 2005 (cf. Figure 8e).

corresponding months of two consecutive years, we can exclude an effect due to seasonal factors, while a modification of superficial roughness and consequently of the geometry of the backscattering surface is more plausible. Besides the nature of this change (e.g. a natural process of surface erosion or debris accumulation rather than an anthropogenic one, such as looting activities), however, possible influence from radar speckle cannot be ruled out completely for this area. Indeed, the presence of sparse pixels with very high (or low) radar backscattering might alter locally the backscattering of one of the scenes (even after the spatial filtering) and result in misleading ratioing maps, where detected changes are the local effect of radar speckle. In general, the interpretation of change patterns with dimensions that reproduce the filtering window (hence, 3 by 3 pixels in this case) are to be considered carefully as they can be the effects of speckle, while patterns with extension larger than the filtering window can be considered more robust.

The latter is the case of the two blue patterns clearly distinguished over the Pirámide Naranja and the southeastern corner of Sector B, and identified by ratioing throughout the entire period of observation, February 2003 to November 2005 (Figure 8e).

Blue areas indicate an increase of  $\sigma^0$  possibly due to the creation of better geometric conditions to the radar backscattering mechanism. While the area of the Pirámide Naranja was subject to excavations by the archaeological mission led by G. Orefici during the years imaged by the ASAR scenes, the blue pattern over the southeastern corner of Sector B is not compatible with legal and authorized digging activities (Figure 9a and b). This SAR-based evidence would confirm the impacts of looting activities over that area previously analysed and measured by Lasaponara *et al.* (2012), who retrieved clear proof of an intensification of illegal digs from 2002 to 2008 by applying spatial autocorrelation statistics on VHR optical imagery.

As a general remark, we have to consider that excavations and consequent exposure of walls and raised anthropogenic structures substantially alter the view scene, and in particular the geometric properties. According to the satellite technical characteristics and its acquisition geometry, such alteration may lead to an increased backscattering coefficient due to the presence of dihedral surfaces generating multiple radar backscattering. Furthermore, we do not have to exclude the contribution of the material properties of the objects brought to light by the excavations, which were previously partially or totally buried.

Although we cannot analyse in more detail the differences of backscattering coefficient between adjacent archaeological structures due to the above-mentioned

limits of spatial resolution, the amplitude change detection maps shown in Figure 8 clearly demonstrate the capability of this amplitude-based processing approach to image, even at the medium resolution, surface changes and modifications induced by human activities.

## Conclusions

The archaeological heritage of the Nasca region was investigated by testing the amplitude-based SAR processing approach discussed by Cigna *et al.* (2013).

The results obtained with ENVISAT ASAR IS2 scenes acquired in 2003–2007 demonstrate the enormous potentials of space radar technologies for archaeological prospection and site condition monitoring, especially with regard to the following three activities:

- (i) recognition and classification of archaeological and, more generally, cultural features based on backscattering coefficient and related surface properties;
- (ii) temporal and spatial assessment of  $\sigma^0$  variations associated to natural and/or human-induced deterioration processes or effects due to environmental/climate factors;
- (iii) mapping of surface changes to perform strategic monitoring of cultural heritage potentially at risk.

Apart from the intrinsic limits of medium resolution SAR imagery, the examples of radar signatures discussed here with regard to the Nazca Lines close to the Panamericana Sur, the *puquios* of Rio Taruga and the archaeological site of Cahuachi confirm that the identification of surface features based on SAR amplitude information is a tool suitable to detect anthropogenic features within the view scene.

As well known, different material properties (e.g. surface roughness, mineralogical composition, moisture content) produce different responses to the incident microwave wavelength. The capability of  $\sigma^0$  values and associated time series extracted from the MLIs to distinguish, for instance, a geoglyph from the surrounding bare soil or a *puquio* from neighbouring vegetation, is further proof that SAR amplitude information can be used effectively in archaeology.

Furthermore, the fact that we can detect the ‘footprints’ belonging to archaeological features even at medium resolutions – supposed to be non-optimal for detailed applications – demonstrates that these historical imagery archives are precious reservoirs of information to study archaeological sites. This also encourages further tests on HR to VHR SAR imagery (e.g. high-resolution SpotLight data from the TerraSAR-X mission).

As was expected, no inferences could be drawn about buried structures over Cahuachi and the northwestern area of the archaeological mounds (Sector B). Nevertheless, the amplitude change detection maps clearly showed the sectors affected by a decrease or increase of backscattering coefficient throughout the period February 2003 to November 2005. The validation of the detected change patterns by means of background knowledge and site conservation history provided evidence on the feasibility of SAR remotely-sensed condition monitoring for the preservation of the archaeological heritage, as well as from damage due to looting activities. While the  $\sigma^0$  changes over the Pirámide Naranja are attributable to the effects of the archaeological excavations contemporary to the acquisition of the processed images, the blue pattern indicating a  $\sigma^0$  change over the southeastern corner of Sector B might be related to illegal excavation, as previously suggested by other remote sensing studies carried out over that area (cf. Lasaponara *et al.*, 2012).

Monitoring of  $\sigma^0$  variations in time is also useful for landscape assessment and preservation of ancient traces of human occupation of the environment, as demonstrated by the amplitude-based recognition of *puquios* in Rio Taruga riverbed and the insights provided into their hydraulic regime and condition. Advantages (and shortcomings) of multispatial scale SAR imagery to contextualize the prospection of archaeological sites in the framework of a broader environmental and landscape assessment are also illustrated and discussed by Cigna *et al.* (2013), in the perspective of a combined study of the cultural and natural heritage of the Nasca region.

## Acknowledgements

The authors thank CNR for supporting the project 'Earth Observation technologies for the survey, the study and the valorization of ancient hydraulic systems' in the framework of the Italian–Peruvian Bilateral Programme and the Italian Ministry of Foreign Affairs for supporting the research activity in the framework of the project 'Diagnostics for the Conservation, Archaeo-geophysics and Risk Assessment of Cultural Heritage in Peru (2012)' of the ITACA Mission. ENVISAT ASAR imagery, auxiliary data and DORIS precise orbits were provided by the European Space Agency to the authors through the Category-1 Project Id. 11073. ASTER multispectral data and GDEM V2 are products of the Ministry of Economy, Trade, and Industry (Japan) and US National Aeronautics and Space Administration, and were made available through the Land Processes Distributed Active Archive Center (LP DAAC) – Global Data Explorer. The ASAR data processing was carried out using the GAMMA SAR and

Interferometry Software, developed by GAMMA Remote Sensing and Consulting AG (Switzerland) and licensed to the British Geological Survey (BGS), Natural Environment Research Council (NERC), UK. This paper is published with the permission of the Executive Director of the BGS, NERC.

## References

- Anselin L. 1995. Local indicators of spatial association LISA. *Geographical Analysis* **27**(2): 93–115.
- ASTER GDEM Validation Team. 2011. ASTER Global Digital Elevation Model Version 2, Summary of Validation Results. 31 August, Ministry of Economy, Trade, and Industry (Japan) and US National Aeronautics and Space Administration.
- Braun M. 2010. *TerraSAR-X image of the month: the Nazca lines in Peru*. News Archive Space, 2 July 2010. [http://www.dlr.de/en/desktopdefault.aspx/tabid-6215/10210\\_read-25333/](http://www.dlr.de/en/desktopdefault.aspx/tabid-6215/10210_read-25333/) (accessed 20 April 2013).
- Cigna F, Del Ventisette C, Gigli G, *et al.* 2012. Ground instability in the old town of Agrigento (Italy) depicted by on-site investigations and persistent scatterers data. *Natural Hazards and Earth System Sciences* **12**: 3589–3603. DOI: 10.5194/nhess-12-3589-2012.
- Cigna F, Tapete D, Lasaponara R, Masini N. 2013. Amplitude change detection with ENVISAT ASAR to image the cultural landscape of the Nasca region, Peru. *Archaeological Prospection* **20**(2): 117–131. DOI: 10.1002/arp.1451.
- Evans LD, Farr TG. 2007. The use of interferometric synthetic aperture radar (InSAR) in archaeological investigations and cultural heritage preservation. In *Remote Sensing in Archaeology. Interdisciplinary Contributions to Archaeology*, Wiseman J, El-Baz F (eds). Springer-Verlag: Berlin; 89–102.
- GAMMA. 2012. *GAMMA SAR and Interferometry Software: Documentation and User Guides*. Software Version. 15 June. GAMMA Remote Sensing AG, Gümligen, Switzerland.
- Lambers K, Sauerbier M. 2006. A fresh view on the Nasca Lines: investigating geoglyph visibility in Palpa (Ica, Peru). In: *Digital Discovery: Exploring New Frontiers in Human Heritage; CAA 2006; Computer Applications and Quantitative Methods in Archaeology; Proceedings of the 34th Conference*, Clark JT *et al.* (eds), Archaeolingua: 228–238.
- Lasaponara R, Masini N. 2012. Following the ancient Nasca *puquios* from space. In *Satellite Remote Sensing. A New Tool for Archaeology*, Lasaponara R, Masini N (eds). Remote Sensing and Digital Image Processing Vol. **16**, Springer-Verlag: Berlin; 269–289.
- Lasaponara R, Masini N, Rizzo E, Orefici G. 2011. New discoveries in the Piramide Naranjada in Cahuachi (Peru) using satellite, ground probing radar and magnetic investigations. *Journal of Archaeological Science* **38**: 2031–2039. DOI: 10.1016/j.jas.2010.12.010.
- Lasaponara R, Danese M, Masini N. 2012. Satellite-based monitoring of archaeological looting in Peru. In *Satellite Remote Sensing. A New Tool for Archaeology*, Lasaponara R, Masini N (eds). Remote Sensing and Digital Image Processing Vol. **16**, Springer-Verlag: Berlin; 177–193.

- Lefort A, Grippa M, Walker N, Stewart LJ, Woodhouse I. 2004. Change detection across the Nasca pampa using spaceborne SAR interferometry. *International Journal of Remote Sensing* **25**(10): 1799–1803. DOI: 10.1080/0143116031000117038.
- Masini N, Lasaponara R, Rizzo E, Orefici G. 2012. Integrated remote sensing approach in Cahuachi (Peru): studies and results of the ITACA Mission (2007–2010). In *Satellite Remote Sensing. A New Tool for Archaeology*, Lasaponara R, Masini N (eds). Remote Sensing and Digital Image Processing Vol. **16**, Springer-Verlag: Berlin; 307–344.
- ONERN. 1971. *Inventario, Evaluación, y Uso Racional de los Recursos Naturales de la Costa: Cuenca del Río Grande (Nazca)*. Oficina Nacional de Evaluación de Recursos Naturales: Lima.
- Orefici G. 2009. Cahuachi, the largest adobe Ceremonial centre in the world. In: *Nasca. El desierto del los Díos de Cahuachi*. Graph: Lima; 36–59.
- Orefici G. 2012. *Capital teocrática Nasca*. Universidad de Porres, Fondo Editorial: Lima.
- Patruno J, Dore N, Crespi M, Pottier E. 2012. A multi-sensor polarimetric analysis over archaeological sites. In *Geoscience and Remote Sensing Symposium (IGARSS)*, IEEE International; 6805–6808. DOI: 10.1109/IGARSS.2012.6352601.
- Reinhard J. 1996. *The Nazca Lines: a New Perspective on their Origin and Meaning*. Los Pinos: Lima.
- Richter C, Teichert B, Hanzalova K, Pavelka K. 2011. The Nasca Project – a German-Czech cooperation. *XXIII International CIPA Symposium*, Prague, September 12–16.
- Ruescas AB, Delgado JM, Costantini F, Sarti F. 2009. Change detection by interferometric coherence in Nasca Lines, Peru (1997–2004). In *Fringe 2009*, 30 November to 4 December, ESRIN, Frascati, European Space Agency SP-677.
- Schreiber KJ, Rojas JL. 2006. *Aguas en el desierto: los puquios de Nasca*. Fondo Editorial, Pontificia Universidad Católica del Perú.
- Silverman H. 1993. *Cahuachi in the ancient Nasca world*. University of Iowa Press: Iowa City.
- Tapete D, Cigna F. 2012. Rapid mapping and deformation analysis over cultural heritage and rural sites based on persistent scatterer interferometry. *International Journal of Geophysics*, Article 618609: 1–19. DOI:10.1155/2012/618609.
- Tapete D, Fanti R, Cecchi R, Petrangeli P, Casagli N. 2012. Satellite radar interferometry for monitoring and early-stage warning of structural instability in archaeological sites. *Journal of Geophysics and Engineering* **9**(4): S10–S25. DOI:10.1088/1742-2132/9/4/S10.
- Tapete D, Casagli N, Fanti R. 2013. Radar interferometry for early stage warning of monuments at risk. In *Landslide Science and Practice*, Margottini C, et al. (eds). Early Warning, Instrumentation and Monitoring Vol. **2**. Springer-Verlag: Berlin; 619–625.